Arch. Metall. Mater. **64** (2019), 2, 739-746

DOI: 10.24425/amm.2019.127607

M. VONČINA*#, J. MEDVED*, L. JERINA*, I. PAULIN**, P. CVAHTE***, M. STEINACHER***

THE IMPACT OF Al-Ti-B GRAIN-REFINERS FROM DIFFERENT MANUFACTURERS ON WROUGHT Al-ALLOY

To investigate the impact of various Al-Ti-B grain-refiners on solidification and grain-refining performance, a wrought aluminium alloy AA6182 was used. Three different grain-refiners from different manufacturers were used to establish the efficiency, i.e. contact time before casting, on the primary solidification and grain formation size. The primary solidification of α-Al grains at inoculation was observed by using thermal analysis (TA). Differential scanning calorimetry (DSC) was used in order to analyze the quality of various grain-refiners. The size of the primary grains was analyzed using optical microscopy (OM). Scanning electron microscopy (SEM) was used to estimate the size and distribution of Al_3Ti and TiB_2 particles in various grain-refiners and to establish the best efficiency of the investigated grain-refiners.

Within 1-4 min of inoculation the smallest fine equiaxed grains were achieved when either one of the investigated grain-refiners was added. It was established, that grain-refiner A contains higher content of impurities which do not melt in the experimental temperature range made by DSC method. The most pure grain-refiner turned out to be grain-refiner B, in which the most optimal number of TiB_2 particles and particle size distribution was found.

Keywords: Al-Ti-B grain-refiners; aluminium alloy AA6182; TiB_2 particles; Al_3Ti particles; inoculation potential

1. Introduction

Grain-refinement has become a standard melt treatment practice in aluminium foundries world-wide with well documented technical and economical advantages. Commercial refiners are manufactured from the Al-Ti-B ternary system, often with more Ti than required to form TiB_2 particles [1]. The vast majority of grain refining applications employ Al-Ti-B alloys which typically contain 2-10 wt.% Ti and 0.1-2 wt.% B [2]. Hence, the microstructure of these alloys typically comprises, in addition to the insoluble TiB_2, the soluble Al_3Ti particles dispersed in an aluminium matrix. The former act as heterogeneous nucleation sites while Al_3Ti particles readily dissolve in the melt and provide solute Ti that partioning between the solid and liquid phases during solidification, and in this way slows down the growth process [2].

The very popular Al-Ti-B refiners are known to perform adequately for wrought aluminium alloys except when the alloy to be inoculated contains one or more of the elements whose borides are more stable than TiB_2. The mutual presence of Al_3Ti and AlB_2 particles in Al-Ti-B alloys, on the other hand, could offer to maximize the grain-refining efficiency for aluminium foundry alloys [3,4,7]. A fine equiaxed grain structure leads to several benefits, such as high yield strength, high toughness, improved machinability and excellent deep drawability of the products [3-5].

Various mechanism for grain refinement involving the addition of Al-Ti-B-based grain-refiners are known: carbide-boride particle theory [8], peritectic theory [9-12], peritectic hulk theory [13,14], hypernucleation theory [15], duplex nucleation theory [16] and solute theory [17-19]. Which mechanism takes place in the grain-refined alloy is hard to predict. One of the major challenges in nucleation research is the experimental difficulties in examining the nucleation process in situ since nucleation occurs in liquid medium at high temperature and in an extremely short time scale. A particularly important aspect of grain-refinement is the crystallographic matching across the solid/substrate interface at the moment of heterogeneous nucleation [3]. A popular grain-refinement mechanism has been proposed as TiB_2 acts as a substrate for the nucleation of Al_3Ti, which then nucleates α-Al grains, i.e., via two steps of heterogeneous nucleation. Without the covering Al_3Ti layer, TiB_2 are easily contaminated by impurities that have a high tendency to form eutectic microstructures with aluminium and therefore being poor in nucleating α-Al grains [20]. However, the Al_3Ti layer must be thinner enough and dynamic to avoid agglomeration to form compounded particles. By considering the high solubility of Al_3Ti in aluminium and less than 0.01 wt. % Ti in solution,

* UNIVERSITY OF LJUBLJANA, FACULTY OF NATURAL SCIENCES AND ENGINEERING, AŠKERČEVA 12, 1000 LJUBLJANA, SLOVENIA
** INSTITUT OF METALS AND TECHNOLOGY, LEPI POT 11, 1000 LJUBLJANA
*** IMPOL GROUP, PARTIZANSKA 38, 2310 SLOVENSKA BISTRICA
# Corresponding author:maja.voncina@omm.ntf.uni-lj.si

a substrate is needed for the nucleation of Al_3Ti in grain-refinement. Therefore, a dynamic layer of Al_3Ti forms on the surface of TiB_2 particles, $(Ti,Al)B_2$ particles precisely, in solidification and then dissolves into α-Al after nucleating α-Al grains, which is supported by a peritectic reaction in an Al-Ti phase diagram [4]. It is found that the quantities of Al_3Ti particles introduced are much lower than those of grains in the as-cast aluminium alloys, while those of introduced TiB_2 are higher. Thus it is concluded that the Al_3Ti particles in the Al-Ti-B grain-refiners cannot be the primary nucleation sites during solidification of aluminium, TiB_2 particles are required [20]. Grain-refiners particles can also nucleate some type of intermetallic phases in 6xxx series of Al-wrought alloys [21].

The ratio between Ti/B in master alloy and the way of processing conditions leads to a different morphologies of the Al_3Ti particles which may be resulted from different growth mechanisms. In various Al-Ti-B grain-refines the morphology of Al_3Ti particles could be as large blocky Al_3Ti particles in the α-Al grain centres while smaller TiB_2 particles being pushed into the grain boundaries (Al-5 wt.% Ti-1 wt.% B) or as flaky when the Ti/B ratio is reduced (Al-3 wt.% Ti-1 wt.% B) [22,23,25]. Ti/B weight ratio corresponding to TiB_2 stoichiometry is 2.215; refining performance improves sharply as this ratio is exceeded, but wanes at higher titanium contents [23,25].

There are many benefits from the use of grain-refiners in aluminium alloy castings. For example, mechanical properties can be improved, susceptibility tendency to hot cracking is reduced and fluidity is improved [26]. However, it is important to design the addition process to achieve the most effective grain-refinement, e.g. finding the contact time with the highest grain-refinement efficiency. If the contact time is too short, the finest grain size may not be achieved. On the other hand, if the contact time is too long, effectiveness of the grain-refiner will be lowered [3,23]. Many researchers have made an assumption that the fading time resulted from the higher density of TiB_2 and Al_3Ti comparing to that of molten aluminium so they settled down at the bottom of the furnace after long contact time.

The present work was undertaken to synthesize an Al-Ti-B alloys which contains both, the insoluble TiB_2 and the soluble Al_3Ti particles and to explore the best potential as a grain-refiner for wrought Al-alloy AA6182. The objectives of the present investigation are to establish the most effective grain-refiner Al-Ti-B of three different manufacturers and to understand the effects of amount of master alloy added and the contact time on the grain-refinement of wrought aluminium alloy AA6182.

2. Materials and methods

The compositions of experimental AA6182 alloy is listed in Table 1 and the grain-refiner Al-Ti-B master alloys designations (named A, B and C), additions and chemical composition, made by Optical emission spectrometer with inductively coupled plasma ICP-OES (Agilent 720) are listed in Table 2. The AA6182 aluminium alloy was melted in an induction furnace in steel crucible coated with BN-foundry coating. The experimental alloy was preheated at 700°C. During the heating and melting the protective gas Ar was purged from the bottom of the steel crucible. When the melting was completed, the Al-Ti-B master alloy was added into the melt, at either 1.2 or 1.5 g/kg. The amounts of master alloy added to the melt in this study were recommendations from the manufacturers. The melt was held for one of seven different contact times (varying from 0 (base alloy), 1, 2, 4, 6, 8 and 10 min). A maximum 10 min contact time was selected as the longest contact time for this study because of the previous reports in various references. The experimental samples were then cast at a temperature of 680-690°C in an Croning measuring cell, whereas the cooling rate was ~7 K/s and cooling curves were recorded. In order to characterize the exact solidification of experimental alloys corresponding first derivatives were obtained from the cooling curves.

The samples for grain size assessment were taken from the specimens after thermal analysis and analyzed in the centre region. Specimens were prepared using a standard metallographic technique. Electropolishing was performed with Barker's reagent (4% HBF_4) to show the grain boundaries. All the samples were examined under polarized light, using Leica MeF4M at 25× magnification. The mean linear intercept technique according to ASTM E112 was used to quantify the grain size.

The DSC tests on all three grain-refiners were carried out with an empty reference corundum pan as scans in a dynamic argon atmosphere. The samples were heated up to 720°C at

TABLE 1

Chemical compositions (wt.%) of the experimental alloy AA6182

Element	Zr	Pb	Zn	Cu	Fe	Mn	Cr	V	Ti	Si	Mg	Al
AA6182	0.209	0.003	0.024	0.046	0.229	0.731	0.341	0.016	0.030	1.149	0.859	rest

TABLE 2

Grain-refiner Al-Ti-B master alloy designations and its chemical composition

Designation	Master alloy	Addition /g/kg Al	Chemical element /wt.%						Ti/B ratio
			Si	Cr	Fe	B	Ti	Al	
A	Al-3Ti-1B	1.2	0.20	<0.01	0.17	0.75	3.1	rest	4.13
B	Al-3Ti-1B	1.2	0.13	<0.01	0.12	0.83	3.1	rest	3.73
C	Al-5Ti-1B	1.5	0.20	<0.01	0.12	0.92	4.8	rest	5.22

10 K/min and then equilibrated at this temperature for 10 min before cooling to room temperature at the same cooling rate, at 10 K/min.

In addition, the grain-refiners were anayzed using JEOL JSM-6500F equipped with EDS, WDS in EBSD analysis techniques in order to analyze the size, shape and distribution of Al_3Ti and TiB_2 particles in investigated grain-refiners.

3. Results and discussion

Thermal analysis was used in order to determine the liquidus (T_L) and solidus temperature (T_S) of base and grain-refined AA6182 alloy. To determine exact characteristic temperatures first derivative of cooling curves was used as shown in Fig. 1a. The letters A, B and C presents the grain-refiner of certain manufacturer and the number next to the letter the contact time before casting. As it can be seen the most effective is the contact time from 1-4 min, whereas the liquidus temperature shifts to higher value when either of three grain-refiners are added in the alloy. The best effect, when grain-refiner A was added, was observed at contact time 1 min (Fig. 1b), whereas when grain-refiner B and C was added at contact time 4 min (Fig. 1c and d). At longer contact times the liquidus temperature starts to decrease, the impact of refiner is decreased in all experimental samples. In table 3 liquidus and solidus temperatures from measured cooling curves are listed.

Fig. 2 presents the micrographs of experimental samples taken in polarized light after etching.

These grain-refiners were tested for their grain-refining performance and were found to be fast acting grain-refiners with a good efficiency. The smallest fine equiaxed grains were achieved within 1-4 min of inoculation when either one of the grain-refiners was added. The first micrograph in Fig. 2 shows typical as-cast microstructures of AA6182 Al-alloy. In this case, the grain size is very large, approximately 420 μm as listed in Table 3. While in the case of adding of experimental grain-refines, the grain size is much finer, from 220-330 μm at all experimental contact times (Fig. 2 and Table 3). An enhanced grain-refining performance was observed in sample B1-B4, whereas the most efficient was grain-refiner B at contact time 1, 2 and 4 min. At longer contact times the grains form bigger again.

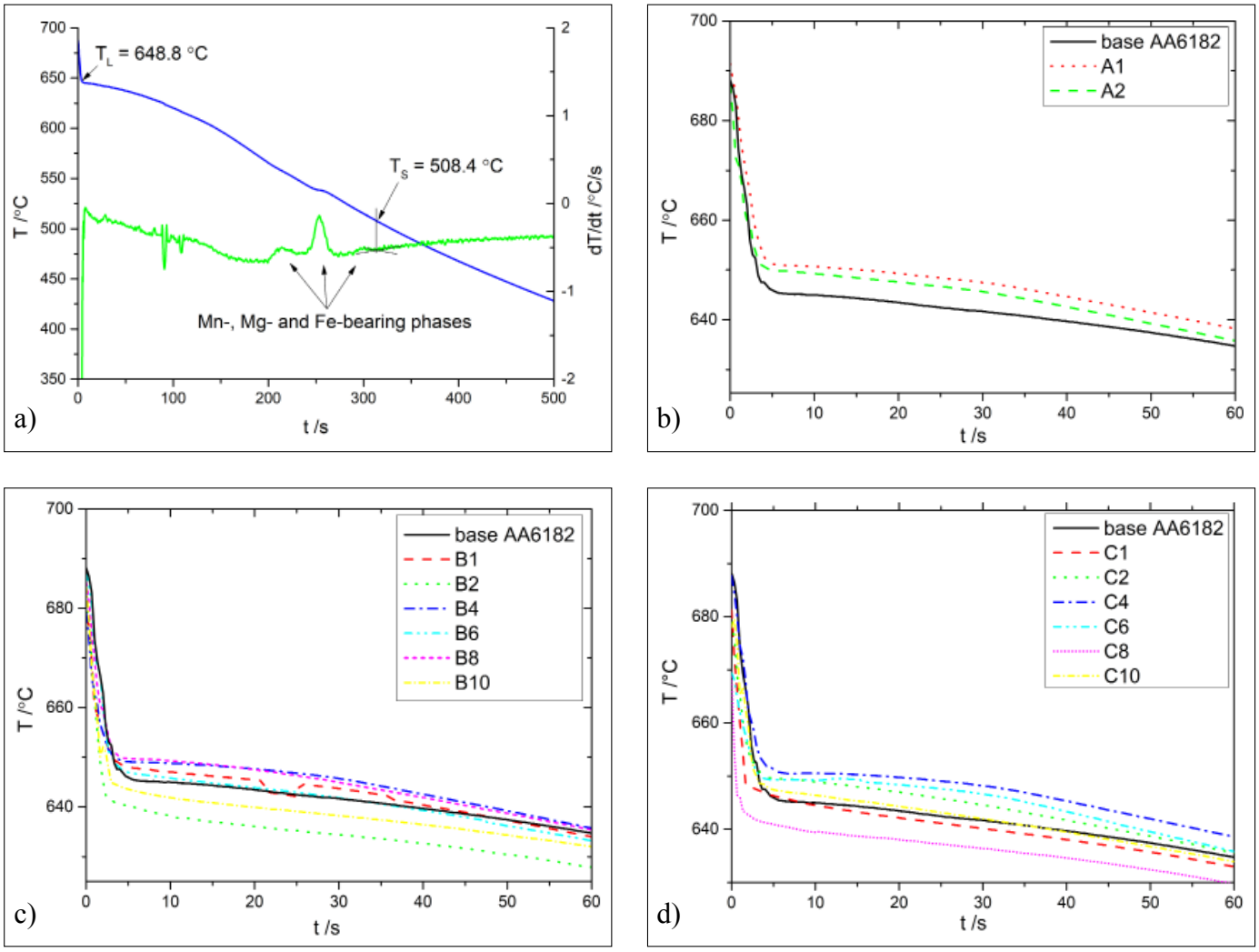

Fig. 1. Cooling curve and its first derivative of base AA6182 alloy, where T_L and T_S are marked (a), cooling curves where the grain-refiner A was added (b), cooling curves where the grain-refiner B was added (c) and cooling curves where the grain-refiner C was added (d)

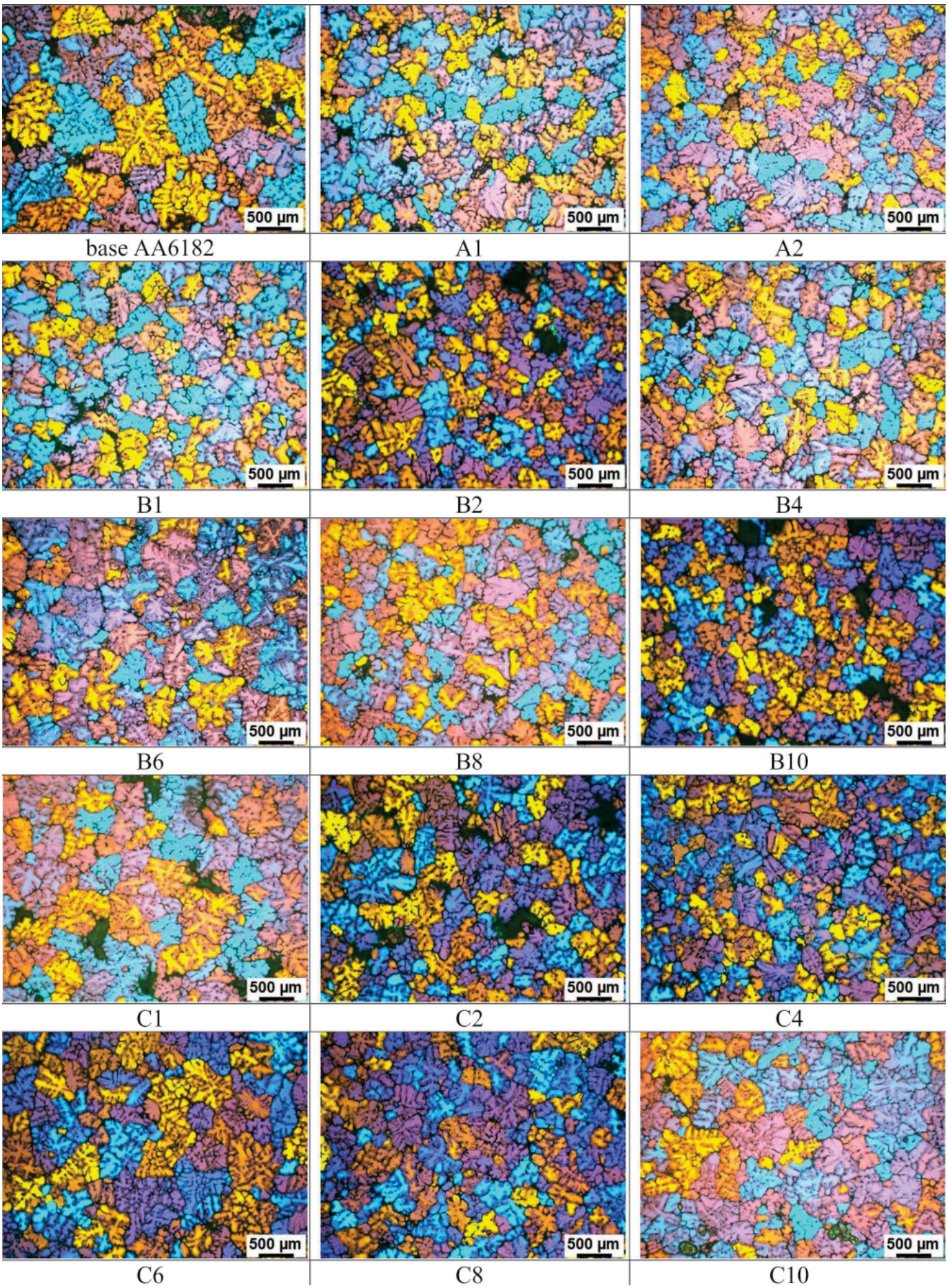

Fig. 2. Micrographs taken in a polarized light for base AA6182 alloy and grain-refined samples at various contact times

TABLE 3

Solidus (T_L) and liquidus (T_S) temperatures /°C determined from cooling curves in Fig. 1 and the grain size (D_{grain}) /μm

Sample	A			B			C		
	D_{grain}	T_L	T_S	D_{grain}	T_L	T_S	D_{grain}	T_L	T_S
base	416.6	649	510	416.6	649	510	416.6	649	510
1	256.2	651	514	216	657	509	257.9	648	506
2	264.6	651	510	237.3	653	510	243.2	652	509
4				250.1	650	507	238.8	652	509
6				293.1	650	506	269.8	650	505
8				280.9	651	507	275.6	646	508
10				247.4	645	506	328.3	650	508

In addition DSC analysis was made to identify the course of melting/solidification of various grain-refiners and to establish the difference between grain-refiners of three different manufacturers. Obvious deviations among the grain-refiners occur on heating (Fig. 3a) and cooling (Fig. 3b) DSC curves. The temperatures of melting and solidifying of all characteristic phases (α-Al, Al_3Ti and $Al_{13}Fe_4$), which could be detected in this temperature range, change when various grain-refiners are tested although the grain-refiner A and B contain approximately the same concentration of Ti and B. Another deviation among the grain-refiners could also be seen, this is melting and solidification enthalpy, whereas it is the lowest at the grain-refiner A. This indicates higher content of impurities as non-metallic inclusion, which do not melt in the experimental temperature range. Inclusions are not so effective inoculants as appropriate combination of Al_3Ti and TiB_2 particles. Moreover, TiB_2 are easily contaminated by impurities, therefore are not efficient as a nucleation sites for α-Al crystal grains.

With an aim to establish the efficiency of various grain-refiners Al-Ti-B, microstructural analysis of all three grain-

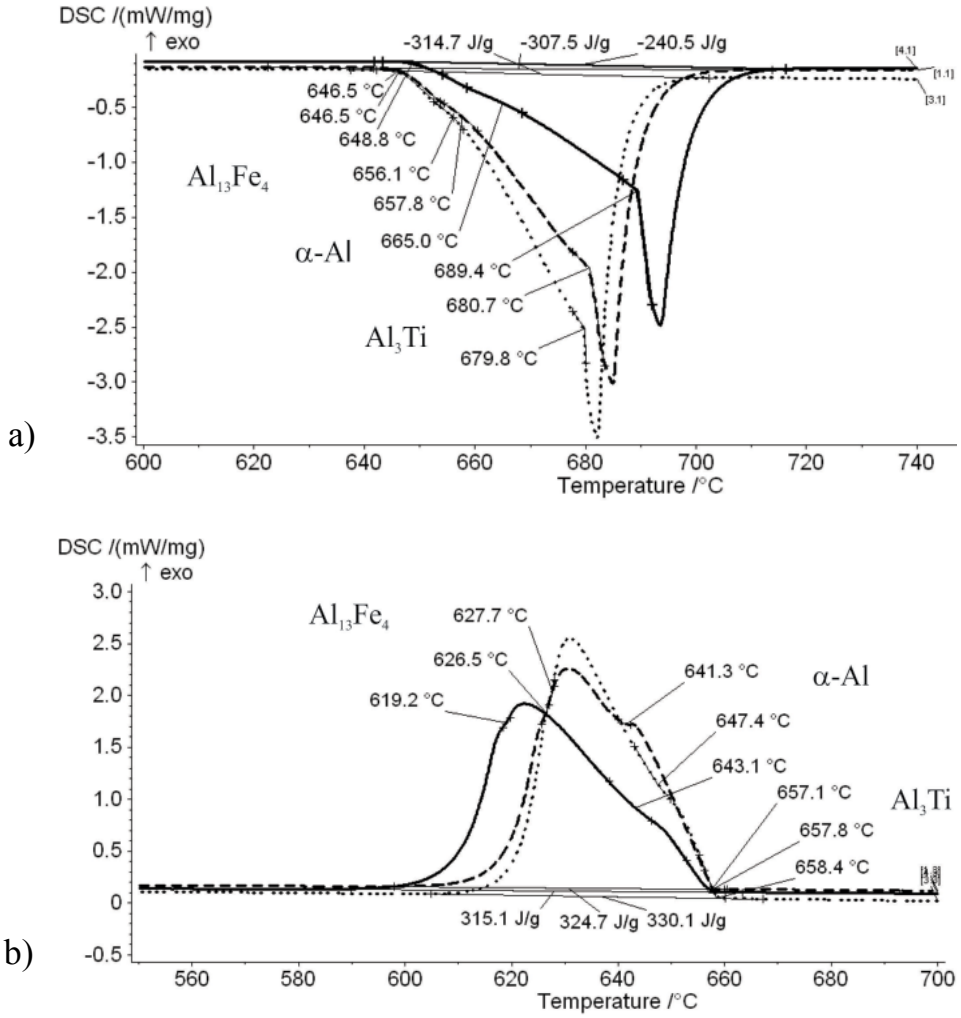

Fig. 3. Heating (a) and cooling (b) DSC curves of three different grain-refiners: A (full line), B (dotted line) and C (stripped line), where the characteristic temperatures and phases are marked

refiners was made. Figs. 4a-c present s typical micro-images of the as-cast grain-refiners. Fig. 4a is from the Al-3 wt.% Ti-1 wt.% B alloy showing large blocky- and flake-like Al_3Ti particles which are unevenly distributed in the matrix, while smaller TiB_2 particles are fragmented in-between. Meanwhile, Fig. 4b shows the Al-3 wt.% Ti-1 wt.% B alloy showing that the morphology of the Al_3Ti particles is much different from grain-refiner A, much more evenly distributed Al_3Ti particles in a flake-like shape can be observed. In case of grain-refiner C (Fig. 4c), Al-5 wt.% Ti-1 wt.% B, the Al_3Ti particles change from blocky to flaky shape when the Ti/B ratio is reduced. The similar observations were reported also by some other researchers [20,21] as already described in the introduction. Both mentioned particles were analysed using SEM, presented in Fig. 5d.

The size distribution of TiB_2 particles in grain-refiners have an essential influence on the grain-refining efficiency. Fig. 5 is showing the number of particles regarding the size (particle surface) in all experimental grain-refiners. Grain-refiner C contains more TiB_2 particles of a very small sizes (from 0.02-0.06 mm^2) than A and B. However grain-refiner C contains also particles of a very larger sizes (0.5-1.25 mm^2). The highest number of TiB_2 particles is in grain-refiner C (33298 per mm^2), but because of unevenly size distribution it is not the most efficient. Grain-refiner B contains almost twice as much particles (11064 per mm^2) as grain-refiner A (6863 per mm^2). This is one more reason for the best results of grain-refinement.

The two different morphologies of the Al_3Ti particles may be resulted from different growth mechanisms and also from different processing conditions. For most effective inoculation insoluble TiB_2 and the soluble Al_3Ti particles in suitable shapes and sizes are needed, while TiB_2 particles act as a substrate for the nucleation of Al_3Ti, where the α-Al nucleates and grow. It is found that the number of Al_3Ti particles introduced into the melt from the addition of Al-Ti-B type grain-refiner have lower influence on the inoculation, than number of TiB_2 particles. This fact leads to a conclusion that grain-refinement by using Al-Ti-B type grain-refiner are not contributed by Al_3Ti particles, but TiB_2 as the primary nucleation substrate while the excess Ti has some effects upon the surface of TiB_2. Nevertheless, Al_3Ti particles in a suitable concentrations and sizes are also needed to achieve the most efficient grain-refining performance.

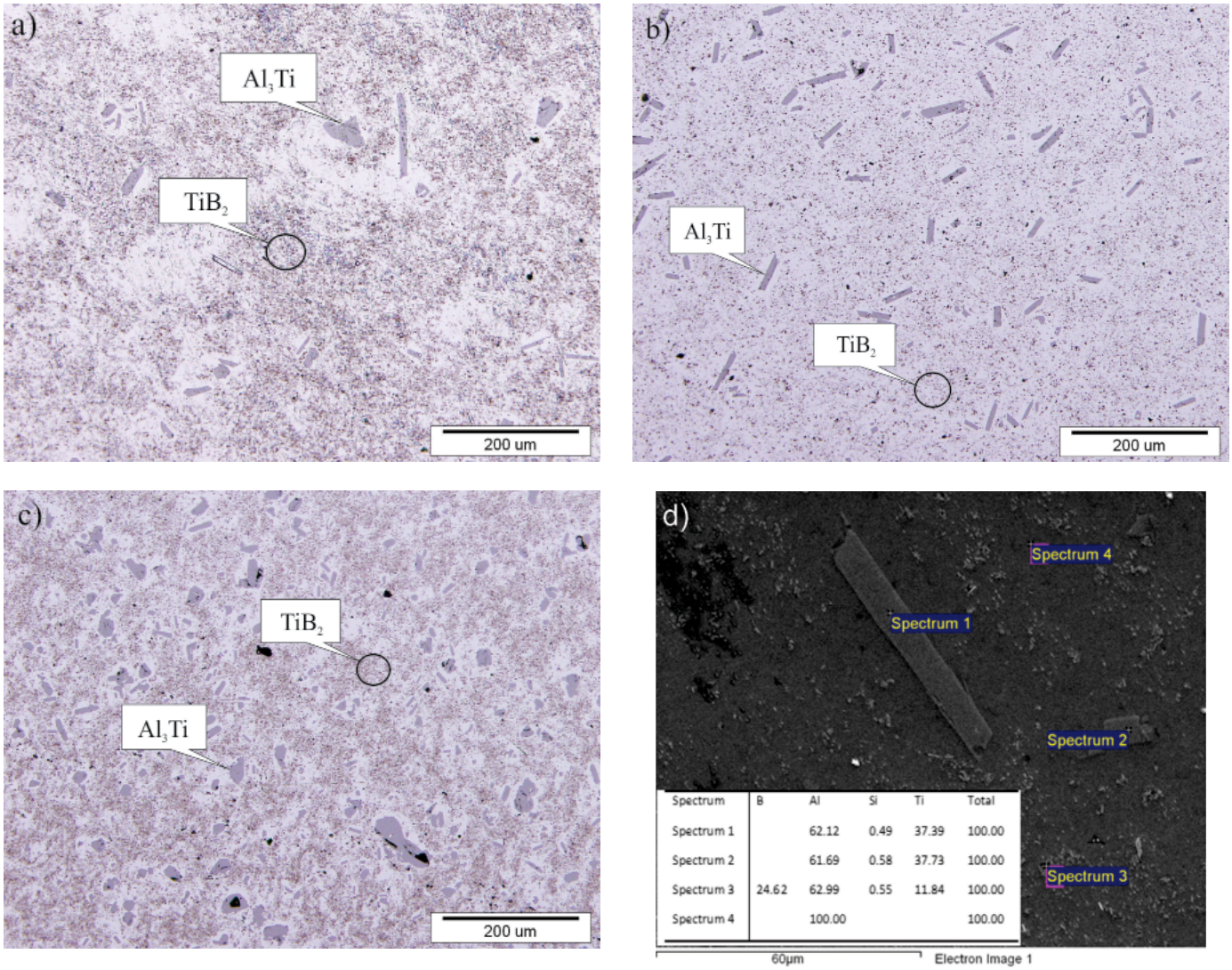

Fig. 4. Micrographs of investigated grain-refiners: A (a), B (b) and C (c); and SEM-image with EDS analysis of Al_3Ti and TiB_2 particles (d)

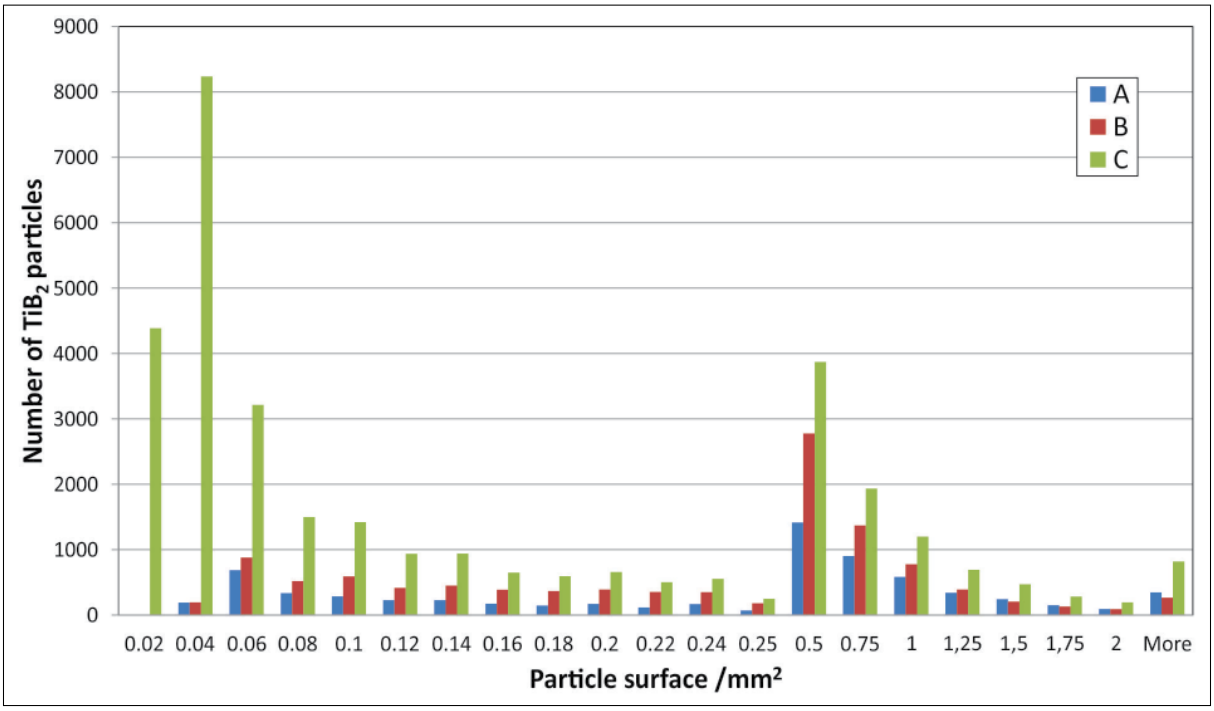

Fig. 5. TiB_2 particle size distribution in various grain-refiners

4. Conclusions

TiB_2 and Al_3Ti form coherent crystallogaphically interface, which promotes the nucleation of Al_3Ti on the surface of TiB_2 particles in an aluminium melt. Without the covering Al_3Ti layer, TiB_2 are easily contaminated by impurities that have a high tendency to form eutectic microstructures with aluminium and therefore being poor in nucleating α-Al grains. In our case presumably latest occurred and following conclusions can be made:

- The smallest fine equiaxed grains were achieved within 1-4 min of inoculation when either one of the grain-refiners was added. An enhanced grain-refinement was observed in sample B1-B4, whereas the most efficient was grain-refiner B at contact time 1, 2 and 4 min. At longer contact times the grains form larger again.
- The melting and solidification enthalpy, analyzed by DSC method, varies regarding the grain-refiner. The lowest was observed at the grain-refiner A, which indicates on a higher content of impurities in the material that do not melt in the experimental temperature range. Inclusions are not so effective inoculants as appropriate combination of Al_3Ti and TiB_2 particles. Furthermore, without the covering Al_3Ti layer, TiB_2 are easily contaminated by impurities that have a high tendency to form eutectic microstructures with aluminium and therefore being poor in nucleating α-Al grains.
- Two different morphologies of the Al_3Ti particles analyzed in this investigation may be resulted from different growth mechanisms and also from different processing conditions. For most effective inoculation insoluble TiB_2 and the soluble Al_3Ti particles in suitable shapes and sizes are needed, while TiB_2 particles act as a substrate for the nucleation of Al_3Ti, where the α-Al nucleates and grow. The most optimal number of TiB_2 particles and particle size distribution was found in grain-refiner B. This is also the reason for the best efficiency of grain-refines B.

Acknowledgements

This work was supported by A Republic of Slovenia, Ministry of Education, Science and Sport and by European Commission, European Regional Development. This work was made in a frame of program Materials and Technologies for New Applications (MARTINA, grand number: C3330-16-529008).

REFERENCES

[1] Y. Birol, Al-Ti-B grain refiners via powder metallurgy processing of Al/K2TiF6/KBF4 powder blends. Journal of Alloys and Compounds **480**, 311-314 (2009).

[2] Y. Birol, A novel Al-Ti-B alloy for grain refining Al-Si foundry alloys. Journal of Alloys and Compounds **486**, 219-222 (2009).

[3] Z. Fan, Y. Wang, Y. Zhang, T. Qin, X.R. Zhou, G.E. Thompson, T. Pennycook, T. Hashimoto, Grain refining mechanism in the Al/Al-Ti-B system. Acta Materialia **84**, 292-304 (2015).

[4] S.A. Kori, B.S. Murty, M. Chakraborty, Development of an efficient grain refiner for Al-7Si alloy and its modification with strontium. Materials Science and Engineering **A283**, 94-104 (2000).

[5] P. Li, S. Liu, L. Zhang, X. Liu, Grain refinement of A356 alloy by Al-Ti-B-C master alloy and its effect on mechanical properties. Materials and Design **47**, 522-528 (2013).

[6] F. Wang, Z. Liu, D. Qiu, J.A. Taylor, M.A. Easton, M.-X. Zhang, Revisiting the role of peritectics in grain refinement of Al alloys. Acta Materialia **61**, 360-370 (2013).

[7] G.S. Vinod Kumar, B.S. Murty, M. Chakraborty, Grain refinement response of LM25 alloy towards Al-Ti-C and Al-Ti-B grain refiners. Journal of Alloys and Compounds **472**, 112-120 (2009).

[8] A. Cibula, The grain refinement of aluminium alloy castings by additions of titanium and boron. J. Inst. Met. **80**, 1-16 (1951).

[9] F.A. Crossley, L.F. Mondolfo, Mechanism of grain refinement in aluminum alloys. AIME Trans. **191**, 1143-1148 (1951).

[10] J.A. Marcantonio, L.F. Mondolfo, Nucleation of aluminium by several intermetallic compounds. J. Inst. Met. **98**, 23-27 (1970).

[11] I. Maxwell, A. Hellawell, A simple model for grain refinement during solidification. Acta Metall. **23**, 229-237 (1975).

[12] I.G. Davies, J.M. Dennis, A. Hellawell, The nucleation of aluminum grains in alloys of aluminum with titanium and boron. Metall. Mater. Trans. B **1**, 275-280 (1970).

[13] M. Vader, J. Noordegraaf, P.C. Van Wiggen, in: E.L. Rooy (Ed.), Light Metals, TMS, Warrendale, PA, 1123-1130 (1991).

[14] L. Backerud, P. Gustafson, M. Johnsson, Grain refining mechanisms in aluminium as a result of additions of titanium and boron. I. Aluminum **67**, 910-915 (1991).

[15] G.P. Jones, in: J. Beech, H. Jones (Eds.), Solidification Processing, Sheffield: University of Sheffield, 496 (1987).

[16] P.S. Mohanty, J.E. Gruzleski, Mechanism of grain refinement in aluminium. Acta Mater. **43**, 2001-2012 (1995).

[17] M. Johnsson, L. Backrud, G.K. Sigworth, Study of mechanism of grain refinement of aluminium after addition of Ti- and B-containing master alloys. Metall. Trans. A **24A**, p. 481 (1993).

[18] K.T. Kashyap, T. Chandrashekar, Effects and mechanisms of grain refinement in aluminium alloys. Bull. Mater. Sci. **24**, 345-353 (2001).

[19] L. Zhou, F. Gao, G.S. Peng, N. Alba-Baena, Effect of potent TiB2 addition levels and impurities on the grain refinement of Al. Journal of Alloys and Compounds **689**, 401-407 (2016).

[20] C.-T. Lee, S.-W. Chen, Quantities of grains of aluminum and those of TiB_2 and Al_3Ti particles added in the grain-refining processes. Materials Science and Engineering **A325**, 242-248 (2002).

[21] G. Sha, K. O'Reilly, B. Cantor, R. Hamerton, J. Worth, Effect of Grain Refiner on Intermetallic Phase Formation in Directional Solidification of 6xxx Series Wrought Al Alloys. Material Science Forum **331-337**, 253-258 (2000).

[22] X. Wang, J. Song, W. Vian, H. M_A, Q. Han, The Interface of TiB_2 and Al_3Ti in Molten Aluminum. Metallurgical and materials transactions B **47B**, 3285-3290 (2016).

[23] P. Schumacher, A.L. Greer, J. Worth, P.V. Evans, M.A. Kearns, P. Fisher, A.H. Green, New studies of nucleation mechanisms in aluminium alloys: implications for grain refinement practice. Materials Science and Technology **14** (5), 394-404 (1998).

[24] Y. Zhang, S. Ji, Z. Fan, Improvement of mechanical properties of Al-Si alloy with effective grain refinement by in-situ integrated Al2.2Ti1B-Mg refiner. Journal of Alloys and Compounds **710**, 166-171 (2017).

[25] H. Yua, N. Wang, R. Guana, D. Tie, Z. Li, Y. Ana, Y. Zhang, Evolution of secondary phase particles during deformation of Al-5Ti-1B master alloy and their effect on -Al grain refinement. Journal of Materials Science & Technology (2018).

[26] C. Limmaneevichitr, W. Eidhed, Fading mechanism of grain refinement of aluminum/silicon alloy with Al/Ti/B grain refiners. Materials Science and Engineering A **349**, 197-206 (2003).